Investigation of Heat Transfer and Nucleate Boiling of Ethanol in Additively Manufactured Cooling Channels

S. Soller[*†], M. T. Scelzo[§], J.-B. Gouriet[§], A. de Crombrugghe[‡], C. Dinescu[#], L. Temmerman[#], A. Doering, S. Schmidt, J. Steelant[°]

*Ariane Group, D-82084 Taufkirchen, Germany

§ Von Karman Institute for Fluid Dynamics, Rhode-St.-Genèse

‡ 3D Systems, Leuven, Belgium

#Cadence Design Systems – Brussels, Belgium

Technical University Munich, Munich, Germany

°European Space Agency, Noordwijk, Netherlands

sebastian.soller@ariane.group

† Corresponding Author

Abstract

Within a joint research project in the GSTP program, a team of industry and academia from Germany and Belgium jointly investigates the effect of surface roughness in additively manufactured cooling channels for rocket engines. To provide a data base for the validation of simulation tools – from simple 1-D engineering correlations to wall-modelled URANS or LES simulations – an experimental setup has been designed, manufactured and commissioned for test. The setup comprises different electrically heated channel floor configurations installed into an optically accessible setup. Ethanol is used as coolant, being a potential rocket propellant itself and having properties similar to hydrazine.

Abbreviations, Acronyms & Symbols

A	Surface area	LOX	Liquid Oxygen	RANS	Reynolds Averaged Navier Stokes
ATV	Automated Transfer Vehicle	m	Mass flow rate	Re	Reynolds number
C_2H_6O	Ethanol	MMH	Monomethylhydrazine	RP	Rocket Propellant 1 (kerosene)
CFD	Computational Fluid Dynamics	NTO	Nitrogentetroxide	RTD	Resistance Temperature Detector
CH_4	Methane	Nu	Nusselt number	Rz	Ten point height of irregularities
c_p	isobaric heat capacity	ONB	Onset of nucleate boiling	T	Temperature
H_2	Hydrogen	OSV	Onset of Significant void	U	Voltage
H_2O_2	Hydrogen peroxide	p	Pressure	URANS	Unsteady RANS
I	Current	P	Power	v	Velocity
k	Thermal conductivity	Pr	Prandtl number	WMLES	Wall-modelled LES
L	Characteristic length	q"	Heat Flux	ξ	Friction coefficient
LES	Large Eddy Simulation	Ra	Roughness average		

1. Motivation and project scope

Regenerative cooling is the standard cooling technique for liquid rocket engines used in launcher propulsion. The cooling systems typically apply rectangular cooling channels on the back side of the combustor, making use of the fins between the cooling channels to enhance the heat transfer from the hot gas wall to the cooling fluid inside the channels in co- or counterflow. For engines operating at moderate system pressure and using hypergolic storable propellants or hydrocarbons like kerosene or ethanol as coolant, the fluid inside the cooling channel typically is in subcritical state in the cooling circuit. As a consequence, forced convection boiling effects can occur, which might not only endanger the structural integrity of the combustion chamber wall, but also may negatively affect the dynamic behaviour of the

injection system, if the two-phase flow persists downstream into the injector head. Therefore, managing the local heat transfer in the cooling system is a key issue for the operation of liquid rocket engines. With the increasing use of additive manufacturing technologies to produce thrust chambers in the 10 kN to 100 kN thrust range, the effect of the comparatively high wall roughness inside the cooling channels on two phase flow phenomena comes into focus.

To investigate these phenomena in detail, an ESA GSTP project performs flow boiling experiments in an optical accessible model channel to investigate in detail the effect of wall roughness on heat transfer and pressure drop inside additively manufactured cooling channels and to provide a data base for the validation of different numerical tools for predicting forced convection boiling phenomena in storable propellant rocket engines. Within the consortium, ArianeGroup acts as prime contractor and coordinator of the project, providing relevant operating conditions for the design of the experiment. The Von-Karman-Institute for Fluid Dynamics (VKI) is responsible for the design and manufacturing of the experiment as well as the performance and evaluation of the experiments. In this task, VKI is supported by 3D Systems, who provided the 3D-printed channel samples. While ArianeGroup uses the data to validate simple and fast engineering models to predict two-phase flow phenomena, Cadence-Belgium and the Chair of Aerodynamics and Fluid dynamics at the Technical University of Munich develop CFD-based models of higher accuracy: Cadence-Belgium develops and assesses modelling strategies, in particular RANS/URANS models with their FINE™/Open with OpenLabs solver, suitable to predict the effect of increased wall roughness on the pressure loss and the heat transfer phenomena in liquid rocket engine cooling channels including the onset of nucleate boiling. TUM performs an analysis of the turbulent flow in AM cooling channels using a Large-Eddy Simulation (LES) in order to understand the flow physics leading to an increased pressure drop and heat transfer enhancement. Since a LES resolving the surface roughness is computationally too expensive, a wall-modelled LES (WMLES) provides a compromise between accuracy by resolving the turbulent large scales and computational effort.

2. Two-phase flow phenomena in liquid rocket engines

2.1 Forced convection boiling

Figure 1 illustrates different boiling regimes in a diagram which shows the wall heat flux as function of the so-called excess temperature, which is the difference between surface temperature and saturation temperature of a fluid for a given pressure $\Delta T_e = T_s - T_{sat}$. The curve has been plotted for water at atmospheric pressure. With increasing excess temperature, the heat flux to the coolant increases linearly up to the onset of nucleate boiling (ONB), at which the heat flux starts to increase more drastically. Further increasing ΔT_e, the nucleation rate of bubbles increases up to a point where the transition to film boiling starts. The heat flux features a local maximum here, the so-called critical heat flux. Increasing the excess temperature further reduces the heat flux transmitted drastically. This drop continues till the Leidenfrost point, which marks the transition end towards full film boiling. This represents a significant risk of overheating of the cooling channels and structural damage. But even before reaching the critical heat flux, boiling phenomena can negatively affect the performance of an engine. The increasing void fraction in the propellant negatively affects the dynamic behaviour in the injector. In different tests performed in the past with the Aestus engine, also in context of the qualification for the ATV missions, nucleate boiling phenomena were recorded during some off-design load points [2].

2.2 Two phase flow in liquid rocket engines

Two-phase flow phenomena can only occur in engines which are operated below the critical pressure of the propellants. Table 1 compares the critical pressure of typical propellants with their corresponding operating pressure. Whereas engines using hydrogen or kerosene as coolant may experience two phase flow phenomena only during transient start-up phases, e.g. during chill-down or immediately after ignition of the engine, LOX/methane engines with a wide throttling range may also feature subcritical cooling conditions at throttled operation, where the chamber pressure and the pressure in the coolant circuit are rather low. For most storable propellants, instead, the operating pressure of typical engines is below the critical pressure. Hence, two phase flow phenomena may occur during steady state operation if the heat load from the combustion chamber wall to the coolant circuit is too high. This also applies to engines being currently under consideration for the use of non-toxic propellant combinations like ethanol as fuel and hydrogen peroxide as oxidiser. Therefore, accurate models to predict the heat transfer phenomena are of key importance for these applications – especially in 3D-printed engines, where the effect of the increased wall roughness on the boiling phenomena is not well investigated. To bridge this gap, an experimental setup has been designed and manufactured which allows to investigate these phenomena for various channel configurations in great detail.
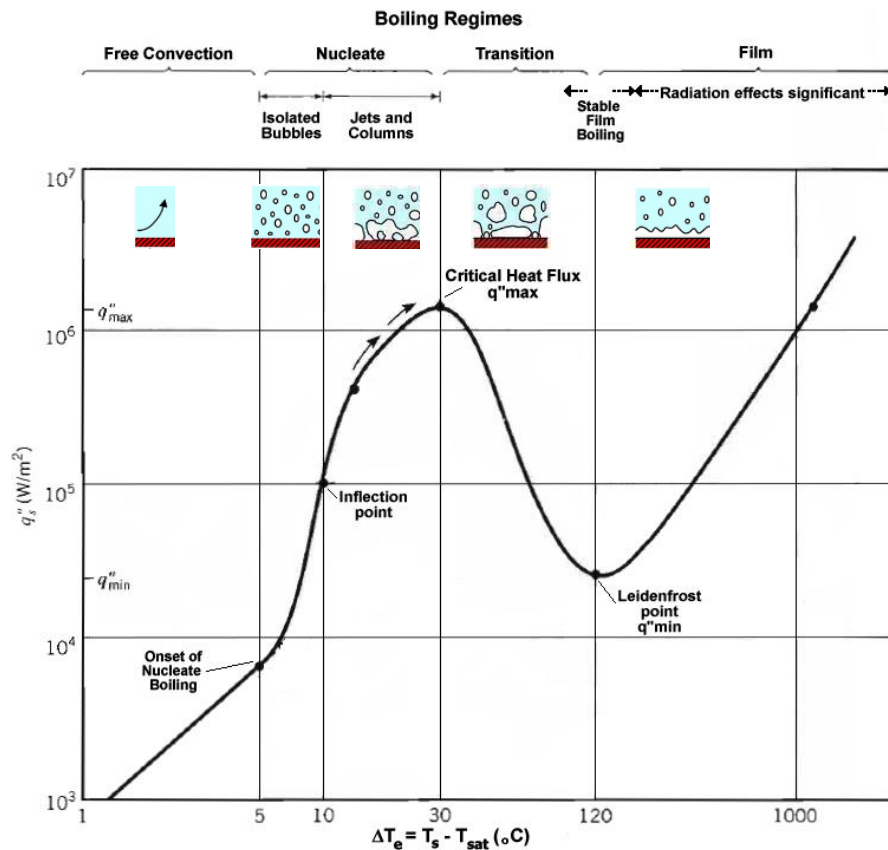
Figure 1: Boiling regimes of water at ambient pressure [1]

Table 1 Critical pressure of propellants compared to typical operating pressure

	H_2	RP-1	CH_4	C_2H_6O	MMH	H_2O_2	N_2O_4
Critical pressure [bar]	13	24	46	63	81	100	101
Operating pressure [bar]	150-300	150-300	30-200	30-70	30-70	30-50	30-70

3. Experimental setup

3.1 Channel setup

The test section is a rectangular mini-channel heated on one side by an electrified metallic floor which is installed into a glass channel (see Figure 2). The thin-walled channel floor (1) is fitted to a housing (2) made of Macor©. This housing itself provides grooves to accommodate O-ring seals and interfaces with a glass channel section (3), which is kept in place by another Brass flange (4). The length of the heated channel floor section is 330 mm.

Electrical power to heat the floor is provided by two electrodes (5). The inlet section and outlet section (6) of the setup have been manufactured be 3D Systems using selective laser melting (SLM). Standard screw-in fittings (7) are used to realise the interface to the test facility's fluid system.

The constant heat power to the test section is supplied with two DC Power supplies from TDK Lambda (ref. GSP-30-340-3P400). They are GENESYS+™ high power GSP programmable DC power supplies with output voltages and currents 16V/800A. With these, a total electrical power of 25 kW can be supplied to the channel floor.

The channel has a width and height of 3 mm x 12 mm and a length of 330 mm. The width of the heated floor section, which is installed along the symmetry plane of the channel, is 6 mm. The channel dimensions resulted from numerous CFD simulations run to assess the effect of the geometry and the heated section on the flow field. Reference [3] provides detailed information on the design study performed to optimise the setup and to enable to build a database free of disturbances by wall effects. Additionally, reference [3] provides information on the CFD models which will be validated with the test data.

In order to assess the effect of the channel surface roughness on the pressure drop and the heat transfer to the coolant, two different channel floor sections have been built. The channel floors have the same dimensions; one of the floors has been machined by milling, whereas the other was not post-processed on the surface meant to be in contact with the coolant (see Figure 3). The measured surface roughness values of both configurations are documented in Table 2.
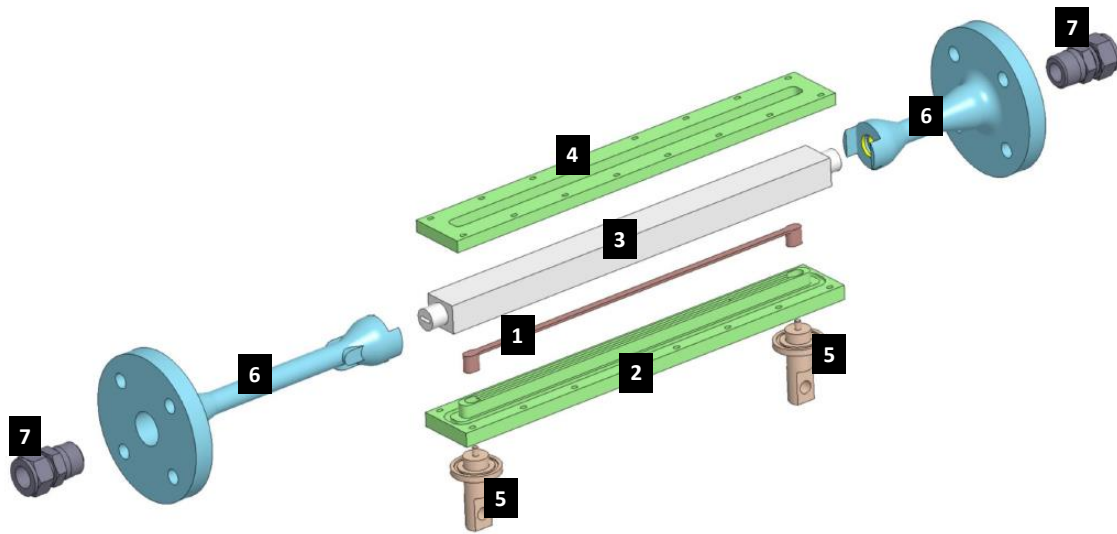
Figure 2: Experimental channel setup

Figure 3: Channel floor sections (AB: as built; M: machined)

Table 2 Surface roughness of channel floor samples

	As built	Machined

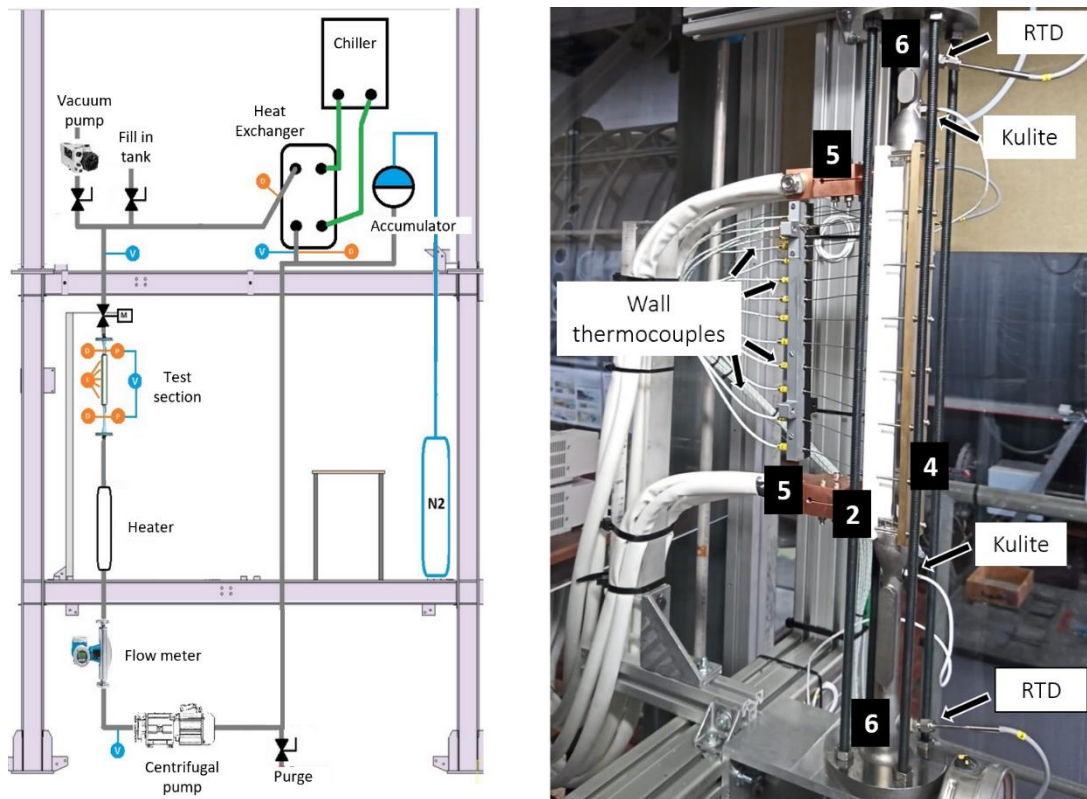|		
Roughness average R_a [μm]	4,52	0,197
Ten point height of irregulartities R_z [μm]	26,11	1,296

Figure 4: Experimental setup: Flow schematic (left) and test section installed (right)

The test section is installed vertically in a dedicated closed loop test facility designed and built at the VKI. Figure 4 (left) shows the closed loop facility and Figure 4 (right) the installation of the channel in the loop, where the numbered labels correspond to the description used in Figure 2. The flow is upward to minimize effects of buoyancy on the boiling behaviour.

The mass flow rate is controlled using a centrifugal pump and a flow regulation valve; the mass flow rate is measured using a Coriolis flow meter. Before the test, the fluid temperature is set by means of the heater. During the experiments, the fluid temperature is further increased in the test; a heat exchanger downstream of the test section brings back the ethanol temperature to the desired inlet value. A membrane-equipped accumulator is used to compensate for the change of fluid density during the test.

3.2 Measurement Setup

The following measurement equipment has been installed to record the required data.

A Yokogawa RCCS34-M01D4SL/LT&S2 Coriolis mass flow meter is sampled at 50 Hz to provide information on the mass flow rate entering the channel. A DP15 Validyne pressure transducer is mounted across the test section to measure the flow pressure drop. Dynamic pressure fluctuations are recorded using Kulite miniature ruggedized high temperature pressure transducers (ref. XTEL-190M-7BARA) installed at the inlet and outlet of the test section.
PT100 resistance thermometers (Tc Direct type 16-1-3.2-4-76-CE2L-R100-1/10-2M RP47) with a diameter of 3.2 mm are installed at the inlet and outlet of the test section to monitor the temperature of the coolant. Type K thermocouples (Tc Direct 12-K-100-321-1.0-2I-3P2LB-2M C40KX-CLASSE 1) are mounted at the channel floor to measure the axial evolution of the wall temperature. Flow visualization will be performed in background light illumination with a high-speed camera Phantom equipped with a Micro Objective Nikon 105 mm focal length.

To acquire additional information on the temperature of the coolant, 2D Laser induced fluorescence (LIF) will be used. In these tests, the coolant will be seeded with temperature sensitive fluorescent dye. While the bandwidth emitted by the fluorescent dye depends on the laser wavelength, the emission intensity depends on concentration, laser intensity and temperature. A ratiometric approach with fluorescence signals acquired in two different bandwidths will allow to eliminate the dependency of the emission from the concentration and laser intensity and increase the sensitivity to the temperature variation. The two bandwidths chosen for these experiments are 540 nm ± 5 nm and 580 nm ± 5 nm. A band stop filter will be used to filter out the laser wavelength (532 nm) from the images.

Preliminary experiments in a small quartz pool have been performed to choose the suitable fluorescent dye (Rhodamine B) and its concentration in ethanol (5 mg/L), the laser (532 nm Litron pulsed laser) and its intensity (95% at 5 Hz), and the two-cameras system (Lavision Davis 8 system with Imager SX4M, 12 bit, 2360x1776 pixels). The field of view with h = 3 mm has been achieved with a Micro Objective Nikon 105 mm, fixed length, f number of 5.6 (depth of field of 0.5 mm).

4. Preliminary results

Currently, the experimental campaign is ongoing. In the following paragraphs, first preliminary results are presented.

4.1 Test procedure and operating conditions

The first set of experiments is being performed with the milled channel floor. Figure 5 shows the temperature evolution at the inlet (TT101) and outlet (TT102) of the test section. During the preparation of the test (0<t<2200s), the heater upstream of the test section and the heat exchanger downstream of the test section are set to provide a constant ethanol temperature at the channel inlet (43°C / 316 K). For the present experiment, the pressure at the inlet of the coolant channel is set to 1.8 bar. The centrifugal pump provides a constant mass flow rate of 0.147 kg/s, resulting in a flow velocity of 5.3 m/s. For these inlet conditions, the corresponding Reynolds number, calculated with the hydraulic diameter of the cooling channel, is $3.6 \cdot 10^4$. Table 3 provides a quick overview on the test conditions. For the present experiment, the setup takes approximately half an hour (or 2000 sec) to reach thermally stable operating conditions.
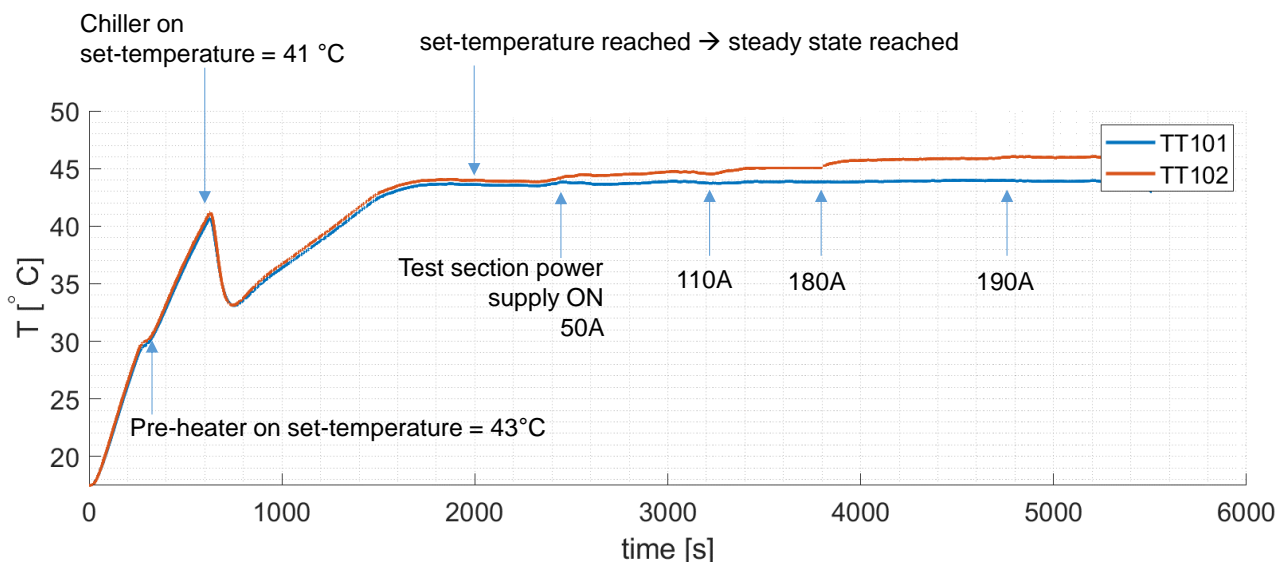

Figure 5: Fluid temperature evolution during experiment

Table 3 Test conditions

T_{in} [°C]	ΔT_{sub} [°C]	p_{in} [bar]	$\dot{m}$ [kg/s]	v [m/s]	Re [-]	P_{el} [W]
43	55	1.8	0.147	5.3	$3.6 \cdot 10^4$	359-1476

Table 4 heating power levels used in tests

Load point	1	2	3	4	5	6	7
P_{el} [W]	359	509	575	771	981	1212	1476

Once these steady state conditions are achieved, the power supply for the cooling channel floor is switched on, passing an electrical current through the channel floor. The power level is increased stepwise afterwards and each power level is kept for at least ten minutes to allow a steady state to establish.

The results presented below have been achieved for a variation of the electrical power provided for heating from 359 W to 1476 W. The electrical power has been calculated as

$$P_{el} = I \cdot U \tag{1}$$

The heat transmitted to the fluid can be calculated from a balance of enthalpy of the fluid between in inlet and outlet of the cooling channel:

$$P_{cool} = \dot{m} \cdot c_p \cdot (T_{out} - T_{in}) \tag{2}$$

The average heat flux transmitted to the fluid was calculated for a reference surface of A = 6 · 330 mm²:

$$q'' = \frac{P_{cool}}{A} \tag{3}$$

Within the first set of tests, seven different heat load levels have been investigated (see Table 4). Using the correlation of Sato [4], the onset of nucleate boiling (ONB) can be expected for a heating power of 700 W. The onset of significant void (OSV) is to be expected at a heating power of 1070 W, if one uses the correlation of Bowring [5].

4.2 Preliminary data analysis

Figure 6 shows the axial evolution of the wall temperature for different heating levels at constant fluid inlet conditions. The position at 0 mm corresponds to the inlet of the test section whereas the heated section extends from 45 mm to 275 mm. The heat flux levels given in the diagram have been calculated using equation (3). The reproducibility of the wall temperature measurements was checked by repeating the experiment at the inlet conditions reported in Table 3 several times. The results of the repeated tests are shown in Figure 7: the wall temperature measurements are highly reproducible, except for some cases with higher heat flux, where a drop in the wall temperature at around 240 mm is not always visible in the same manner. For the following illustration of these preliminary results, only two wall temperature measurements have been used, at 190 mm (Position 5) and 220 mm (Position 6), as indicated by the red rectangle in Figure 7.
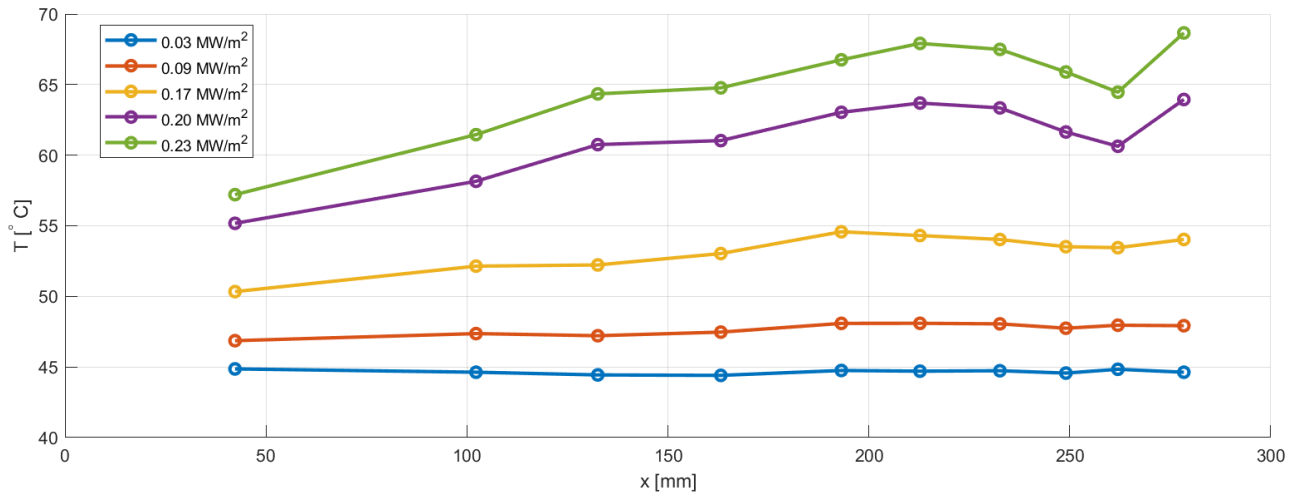
Figure 6: Wall temperature evolution for different heat flux levels
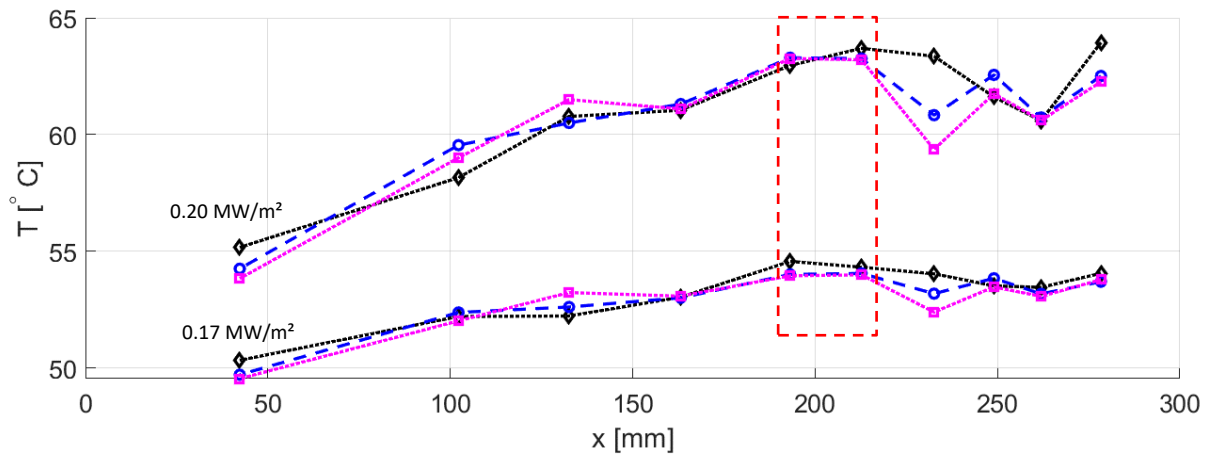

Figure 7: Repeatability of wall temperature measurements for two test cases

Table 5 Comparison of heating power provided and heat pick up by coolant

Load	1	2	3	4	5	6	7
P_{el} [W]	359	509	575	771	981	1212	1476
P_{cool} [W]	264	391	467	612	759	934	1129
Diff [%]	26.5	23.2	18.8	20.6	22.6	22.9	23.5

Table 5 compares the P_{el} and P_{cool} for each power load. A difference of around 23% indicates significant thermal losses due to the Macor block and the quartz channel not fully insulating the setup towards the ambient. Therefore, the following results have been derived considering the heat pickup measured by the enthalpy balance.

As first plausibility check, the flow heat transfer coefficient h was calculated based on the measured enthalpy increase of the fluid as:

$$h = \frac{q''}{(T_{wall} - T_{bulk})}$$ (4)

where the wet wall temperature T_{wall} has been estimated with the 1D conduction equation solved across the metallic channel floor.

This result has been preliminarily compared to the value of h^* derived with the Gnielinsky Nusselt (Nu) correlation (reported for example in [6]) according to the simplified equation (5):

$$Nu = \frac{\frac{\xi}{8} \cdot (Re - 1000) \cdot Pr}{1 + 12.7\sqrt{\frac{\xi}{8}}\left(Pr^{\frac{2}{3}} - 1\right)} \qquad \rightarrow h^* = \frac{Nu \cdot k}{L} \tag{5}$$

where Re and Nu have been calculated with the channel height as reference length.

Table 6 Heat transfer coefficients

Test run	$h_{exp, Pos5}$ [W/m²K]	$h_{exp, Pos6}$ [W/m²K]	h^* [W/m²K]
1	8682	8801	
2	7715	7684	8072
3	7747	7707	

Table 6 compares the value of h* calculated according to equation (5) with the experimental results, as in (4), for the three repeatability experiments. Beside a fairly good comparison with the literature correlation (4% - 9% deviation, to be confirmed with a larger experimental sample), the results show a remarkable repeatability in the heat transfer coefficient derivation with a maximum 15% variation among the repeatability tests.

Figure 8 shows the calculated heat pick up by the coolant P_{cool} compared to the estimated values for onset of nucleate boiling (ONB) and onset of significant void (OSV). According to the literature estimates, boiling phenomena should appear at a heat load of 700 W, corresponding to load point 5 (as referred to in Table 5). In fact, an analysis of the dynamic pressure signal recorded at the channel inlet and outlet shows a significant increase in the signal's standard deviation starting from load point 5 (see Figure 9). Whereas the increase in noise in the first four load points may be attributed to an increase in turbulence induced by the convective heat transfer, the drastic increase in load points 5 – 7 clearly correlates with the onset of nucleate boiling, which was also observable form the high-speed videos, which are currently being post-processed.
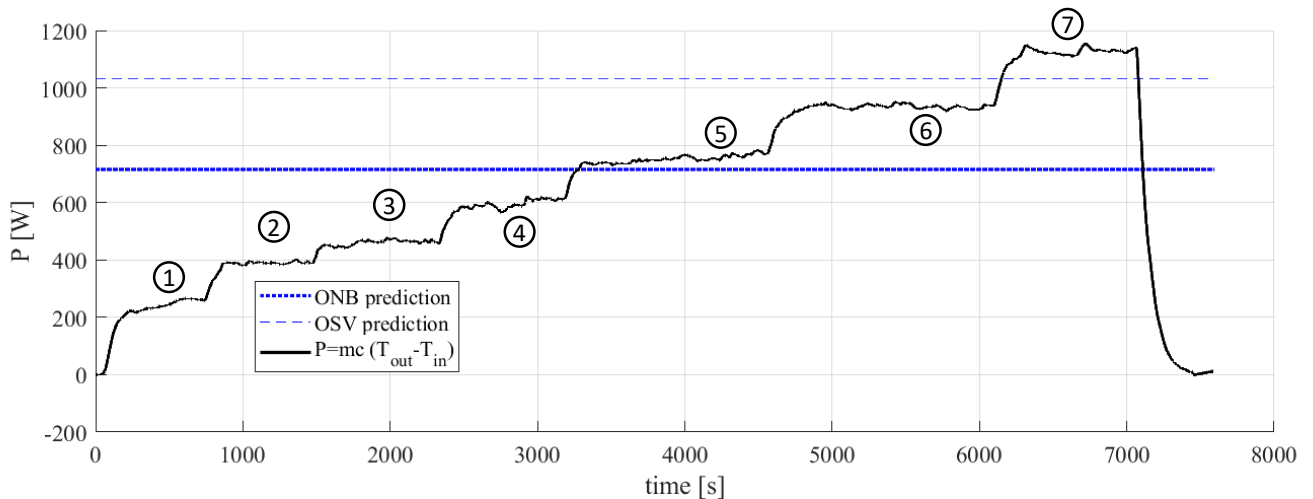

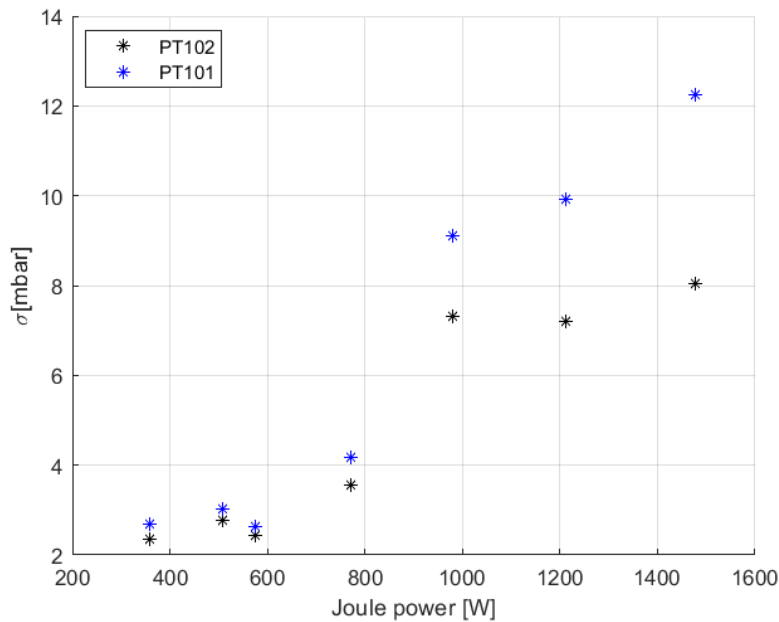Figure 8: Comparison of heat pick-up with ONB and OSV values

Figure 9: Standard deviation of dynamics pressure signal at inlet and outlet of channel

5. Summary

Within joint research project in the GSTP program, a team of industry and academia from Germany and Belgium jointly investigates the effect of surface roughness in additively manufactured cooling channels for rocket engines. To provide a data base for the validation of simulation tools – from simple 1-D engineering correlations to wall-modelled URANS or LES simulations – an experimental setup has been designed, manufactured and commissioned for test. The setup comprises different electrically heated channel floor configurations installed into an optically accessible setup. Ethanol is used as coolant, being a potential rocket propellant itself and having properties similar to hydrazine.

First experiments have been performed to commission the setup using a classically machined channel floor. Test data recorded so far show good agreement with expected values of heat flux for the onset of nucleate boiling. In future tests, the scope of operating conditions will be expanded, and optical diagnostics will be used to acquire additional information on the flow phenomena in the channel. Finally, the tests will be repeated with a channel floor in its "as-built" configuration in order to quantify the effect of surface roughness on pressure drop and heat transfer characteristics.

References

[1] https://en.wikipedia.org/wiki/Nucleate_boiling
[2] ARTA Test Campaign Report, A5-RE-1921-C-2051-MBBO, Airbus Defence and Space, 27.11.2014
[3] Soller, S. Grauer, F., Vollmer, K., Zeiss, W., Scelzo, M.T., Gouriet, J. B., de Crombrugghe, A., Claramunt, K., Dinescu, C., Temmermann, L., Doering, A., Schmidt, S. and Steelant, J. Heat Transfer Phenomena in Additively Manufactured Cooling Channels, SPC2022_00218, 8th Space Propulsion Conference, 09-13 May 2022, Estoril, Portugal
[4] T. Sato and H. Matsamura, "On the conditions of incipient subcooled-boiling with forced convection." Bulletin of JSME , vol. 26, no. 7, pp. 392-398, 1964.
[5] R. W. Bowring, "Physical model, based on bubble detachment, and calculation of steam voidage in the sub-cooled region of a heated channel.," OECD Halden Reaktor Prosjekt, 1962.
[6] Bejan, Adrian, and Allan D. Kraus, eds. *Heat transfer handbook*. Vol. 1. John Wiley & Sons, 2003.